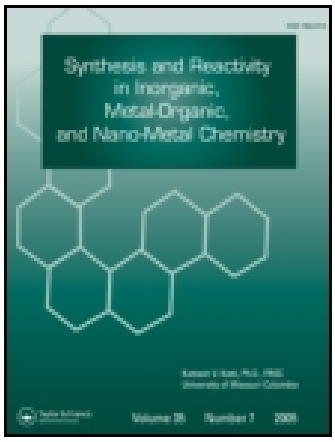

Synthesis and Reactivity in Inorganic, Metal-Organic, and Nano-Metal Chemistry

Publication details, including instructions for authors and subscription information:
http://www.tandfonline.com/loi/lsrt20

A Simple Sonochemical Route for Synthesis Silver Selenide Nanoparticles From $SeCl_4$ and Silver Salicylate

Maryam Jafari[a], Masoud Salavati-Niasari[ab], Kamal Saberyan[c] & H. Sabarou[d]

[a] Department of Inorganic Chemistry, Faculty of Chemistry, University of Kashan, Kashan, I. R. Iran

[b] Institute of Nano Science and Nano Technology, University of Kashan, Kashan, I. R. Iran

[c] Fuel Cycle Research School, NSTRI, Tehran, I. R. Iran

[d] School of Metallurgy and Materials Engineering, Faculty of Engineering, University of Tehran, Tehran, I. R. Iran

Accepted author version posted online: 23 Jan 2014.Published online: 14 Aug 2014.

To cite this article: Maryam Jafari, Masoud Salavati-Niasari, Kamal Saberyan & H. Sabarou (2015) A Simple Sonochemical Route for Synthesis Silver Selenide Nanoparticles From $SeCl_4$ and Silver Salicylate, Synthesis and Reactivity in Inorganic, Metal-Organic, and Nano-Metal Chemistry, 45:1, 58-67, DOI: 10.1080/15533174.2013.818033

To link to this article: http://dx.doi.org/10.1080/15533174.2013.818033

Synthesis and Reactivity in Inorganic, Metal-Organic, and Nano-Metal Chemistry (2015) 45, 58–67

ISSN: 1553-3174 print / 1553-3182 online
DOI: 10.1080/15533174.2013.818033

Taylor & Francis
Taylor & Francis Group

A Simple Sonochemical Route for Synthesis Silver Selenide Nanoparticles From $SeCl_4$ and Silver Salicylate

MARYAM JAFARI[1], MASOUD SALAVATI-NIASARI[1,2], KAMAL SABERYAN[3], and H. SABAROU[4]

[1]*Department of Inorganic Chemistry, Faculty of Chemistry, University of Kashan, Kashan, I. R. Iran*
[2]*Institute of Nano Science and Nano Technology, University of Kashan, Kashan, I. R. Iran*
[3]*Fuel Cycle Research School, NSTRI, Tehran, I. R. Iran*
[4]*School of Metallurgy and Materials Engineering, Faculty of Engineering, University of Tehran, Tehran, I. R. Iran*

Received 15 May 2013; accepted 11 June 2013

For the first time, silver salicylate marked as [Ag(HSal)] was applied to fabricate silver selenide nanoparticles. This article describes a simple approach based on reaction between silver salicylate as an inorganic precursor, $SeCl_4$, and hydrazine hydrate ($N_2H_4.H_2O$) via sonochemical route for the fabrication of silver selenide (Ag_2Se) nanoparticles. The effect of preparation parameters such as pH, ultrasonic power, and reaction temperature on the morphology of the final products was investigated. Ag_2Se nanoparticles were characterized by X-ray powder diffraction (XRD), transmission electron microscopy (TEM), scanning electron microscopy (SEM), and X-ray energy dispersive spectroscopy (EDS).

Keywords: nanoparticle, silver selenide, silver(I) salicylate, ultrasonic irradiation

Introduction

Silver chalcogenides, particularly Ag_2Se, have attracted much attention because of their promising optoelectronic and thermoelectric properties and their application in photovoltaic cells, photoconductors, IR detectors, magnetic field sensors, solid state electrochemical sensors, optical filter, and superionic conductors.[1–6] Ag_2Se, which is a narrow band gap group I–VI compound semiconductor with an energy band gap ~0.15 eV for low temperature phase, has become a material of much research interest in recent years.[7] Up to now there are no reports on the synthesis of Ag_2Se, from organometallic precursors.

To date, silver selenides have been prepared by various methods, such as heating the mixture of the Ag and Se at high temperature,[8] microwave radiation,[9] mechanical alloying of Ag and Se with a high energy ball mill,[10] molecular precursor methods,[11,12] hydrothermal,[13] electrochemical route,[14] sonochemical reaction,[15] organo-selenium precursor,[16] cation exchange reaction using water-dispersed ZnSe nanocrystals as precursors,[17] solid-state reaction of sequentially deposited Ag and Se,[18] and pulse electrodeposition from a single aqueous solution of Ag and Se ions.[19]

The previous methods usually require the combination of higher temperature, higher pressure, inert atmosphere, and long time. Among different methods for synthesis of silver selenides, we have choosen sonochemical method for its rapid reaction rate, controllable reaction conditions and the ability to form nanoparticles with uniform shapes, narrow size distributions, and high purity. The ultrasonic radiation on chemical reactions creates a very instantaneously high temperature and pressure, which develop in and around the collapsing bubble. These conditions formed in the hotspots have been experimentally determined, with transient temperatures of ~5000 K, pressures of 1800 atm, and cooling rates in excess of 10^{10} K/s. As a result, sonication provides an ideal atmosphere for the preparation of nanomaterials.[20–22] For a few years, our group has been interested in the synthesis of nanoparticles using the sonochemical method.[23–26]

To our knowledge, there is no report on the synthesis of Ag_2Se nanoparticles from inorganic precursors. For the first time, we synthesized Ag_2Se nanoparticles by silver salicylate ([Ag(HSal)]) as a coordination compound via sonochemical route. $SeCl_4$ was selected in our experiments to provide a highly reactive selenium source in aqueous solution. In other reports, Se powder was used to produce metal selenides. But Se powder has low reactivity, hence researchers use Na_2SeSO_3 solution. The solution of sodium selenosulfate is relatively unstable. It was obtained by adding selenium powder to a hot solution of sodium sulfite under strring for 1 h at

Address correspondence to Masoud Salavati-Niasari, Department of Inorganic Chemistry, Faculty of Chemistry, University of Kashan, Kashan, P. O. Box. 87317–51167, I. R. Iran. E-mail: salavati@kashanu.ac.ir
Color versions of one or more of the figures in this article can be found online at www.tandfonline.com/lsrt.

Table 1. The reaction conditions of the samples synthesized in this work.

Morphology	Ultrasound temperature (°C)	Ultrasound power (W/cm ^{2})	pH	Ag/Se ratio	Precursor	Sample
Aggregated nanostructures	25	45	—	1:1	$AgNO_3$+$SeCl_4$	1
Nanosphere	25	45	5	1:1	[Ag(HSal)]+$SeCl_4$	2
Nanoparticle	25	45	10	1:1	[Ag(HSal)]+$SeCl_4$	3
Nanoparticle	25	55	5	1:1	[Ag(HSal)]+$SeCl_4$	4
Nanoparticle	25	65	5	1:1	[Ag(HSal)]+$SeCl_4$	5
Nanoparticle	10	55	5	1:1	[Ag(HSal)]+$SeCl_4$	6
Nanoparticle	45	55	5	1:1	[Ag(HSal)]+$SeCl_4$	7
Nanoparticle	65	55	5	1:1	[Ag(HSal)]+$SeCl_4$	8
Aggregated nanospheres	25	45	5	2:1	[Ag(HSal)]+$SeCl_4$	9
Aggregated nanostructures	—	—	5	1:1	[Ag(HSal)]+$SeCl_4$	#10

#Blank Test

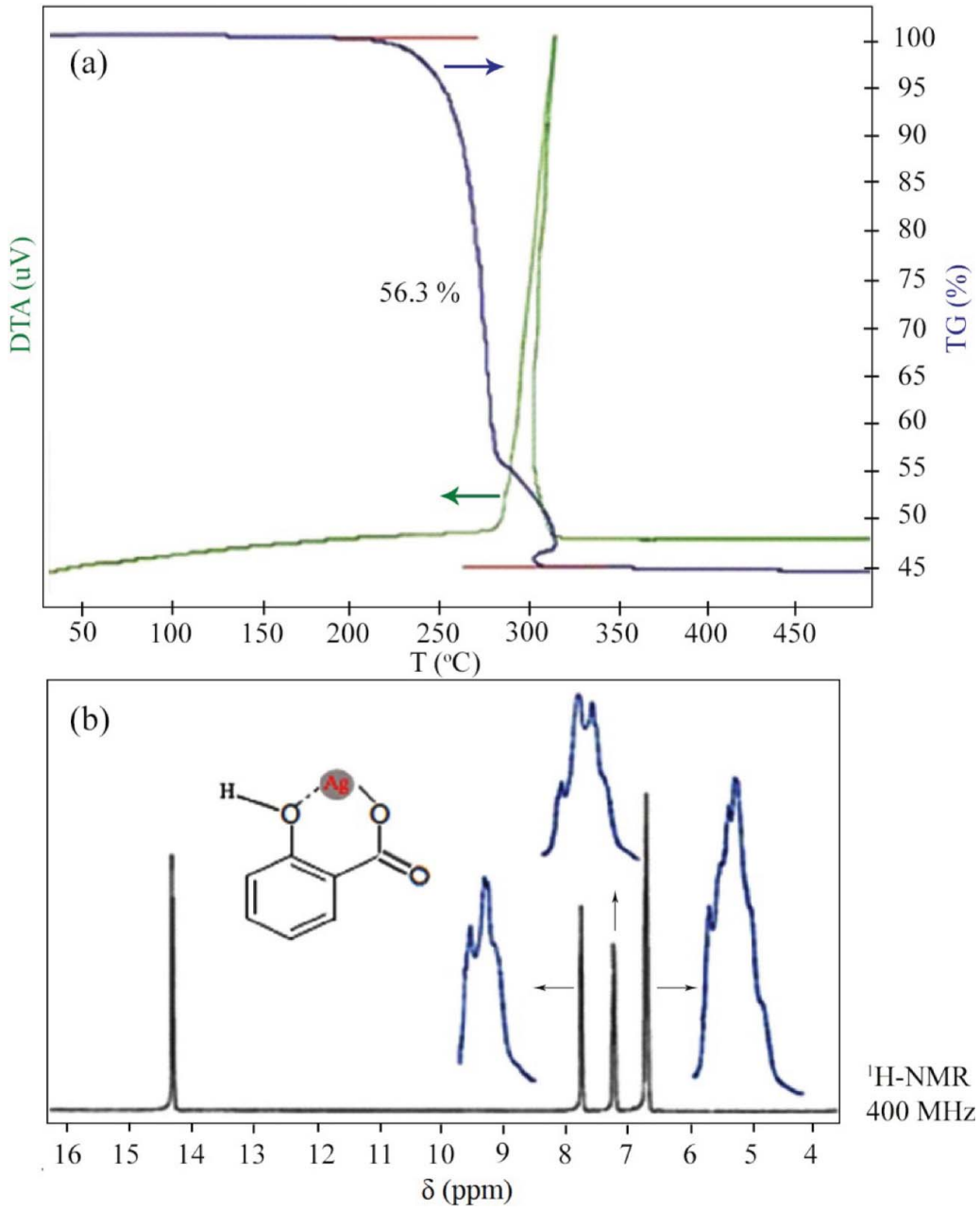

Fig. 1. (a) TGA/DTG/DTA curves of [Ag(HSal)] precursor. (b) ^{1}H-NMR spectrum of [Ag(HSal)] precursor.

90°C and filtering the excess of selenium powder.[27] This process requires long time and high temperature. So, the amount of substance and energy was not economized. In this work effects of different parameters, such as pH, reaction temperature, ultrasound power, and mole ratio of precursors on products morphology were investigated.

Experimental

Chemicals and Equipment

All the reagents were of the commercial available purity. A multiwave ultrasonic generator (Sonicator 3000; Bandeline, MS 72, Germany), equipped with a converter/transducer and titanium oscillator (horn), 12.5 mm in diameter, operating at 20 kHz was used for the ultrasonic irradiation. All ultrasonication experiments were carried out at ultrasonic power between 100–110 mW measured by calorimetry.[28] The XRD of products was recorded by a Rigaku D-max C III XRD using Ni-filtered Cu K_α radiation. SEM images were obtained on Philips XL-30ESEM equipped with an energy dispersive X-ray spectroscopy. TEM images were obtained on a Philips EM208 transmission electron microscope with an accelerating voltage of 200 kV. The EDS analysis with 20 kV accelerated voltage was done. The electronic spectrum of the samples was taken on a Scinco UV–Vis (ultraviolet-visible) scanning spectrometer (Model S-4100). The thermogravimetric analysis and differential thermal analysis (TGA/DTA) of silver salicylate was carried out with Pyris Diamond Perkin Elmer under air atmosphere at a heating rate of 10°C/min from room temperature to 500°C. The reaction conditions of the samples synthesized in this work are shown in Table 1.

Synthesis of [Ag(HSal)] Precursor

Silver(I) salicylate, [Ag(HSal)], was prepared according to the procedure described previously.[29] 2 mmol of $AgNO_3$ was dissolved in 40 mL of distilled water. A stoichiometric amount of sodium salicylate dissolved in an equal volume of distilled water was added dropwise into the solution under magnetic stirring. The solution was stirred about 30 min and a white precipitate was obtained, isolated, and washed with distilled water and ethanol several times to remove impurities, and then dried at 50°C in vacuum.

Synthesis of Nano-Sized Ag_2Se

In a general procedure, nano-sized Ag_2Se was prepared by reacting between [Ag(HSal)] and $SeCl_4$ precursors with molar ratio of 1:1. At first, 0.004 mmol [Ag(HSal)] was dissolved in 100 mL of distilled water then, an appropriate amount of hydrazine was added dropwise to the aqueous solution of $SeCl_4$. After stirring for 20 min, the solution was added to the [Ag(HSal)] solution under strong magnetic stirring at room temperature. Then the solution was irradiated with an ultrasonic horn for 30 min. After cooling to room temperature, the black precipitates were centrifuged, washed by distilled water and ethanol in sequence, and dried in vacuum at 60°C.

Results and Discussion

Thermogravimetric analysis (TGA) and differential thermal analysis (DTA) help to determine the coordinated number or crystallization water molecules of silver salicylate complex. Figure 1 shows TGA, and DTA curves of [Ag(HSal)], which were carried out between 30 and 500°C in air. In the TGA curve, two weight loss steps were observed. According to TGA results, the first weight loss occurred in 276.9°C, and another weight loss shown at 313.8°C was corresponding to silver salicylate decomposition to AgO and Ag_2O, respectively. The weight loss steps with a total mass loss of 56.3% (calcd. 55.80%) are shown as an exothermic stage in the DTA curve presented in Figure 1. According to the mass loss calculations the final decomposition products were AgO and Ag_2O. At high temperature (up to 320°C), a backward movement was seen in the TGA curve of silver salicylate (Figure 1). This phenomenon may be related to the generation of an inert atmosphere of product gas in the crucible, which drove out O_2 gas for a while, causing the formation of some metal or lower valence oxides. When oxygen diffused again in the crucible, the metal or lower oxide oxidized to the normal oxide.[30] Figure 1 shows the proton nuclear magnetic resonance (^{1}H-NMR) spectrum of precursor. The multiple peaks appeared at the chemical shifts of 6.6–7.8 ppm that could be assigned to aromatic protons. The sharp peak appeared at 14.35 ppm could be assigned to the proton of phenolic hydroxyl group. The chemical shift of hydroxyl group showed that this group could interact with silver ion.

The morphology and structure of the resulting samples were investigated by SEM images. Figure 2 shows SEM images of samples synthesized using $AgNO_3$ after 30 min of sonication (sample no. 1). It is clear that aggregated nanostructures are formed in the presence of $AgNO_3$ as Ag source (Figure 2).

Figure 2 indicates that the morphology, grain size, and agglomeration of the nanoparticles were greatly influenced by [Ag(HSal)] as Ag source due to the structure of [Ag(HSal)] complex which contains high steric hindrance surrounds the Ag center. The structure around Ag atoms plays the surfactant role and giving rise to tiny Ag_2Se nanoparticles.[31]

XRD pattern of synthesized Ag_2Se nanoparticles which [Ag(HSal)] was as Ag source (sample no. 2) is shown in Figure 3. The diffraction peaks of the products in Figure 3 can be indexed to orthorhombic Ag_2Se (space group 19/m, JCPDS card 24-1041). No remarkable diffractions of other phases such as selenium, silver, or other compounds can be found in Figure 3, indicating that pure Ag_2Se nanoparticles were synthesized. The sharp diffraction peaks indicate the

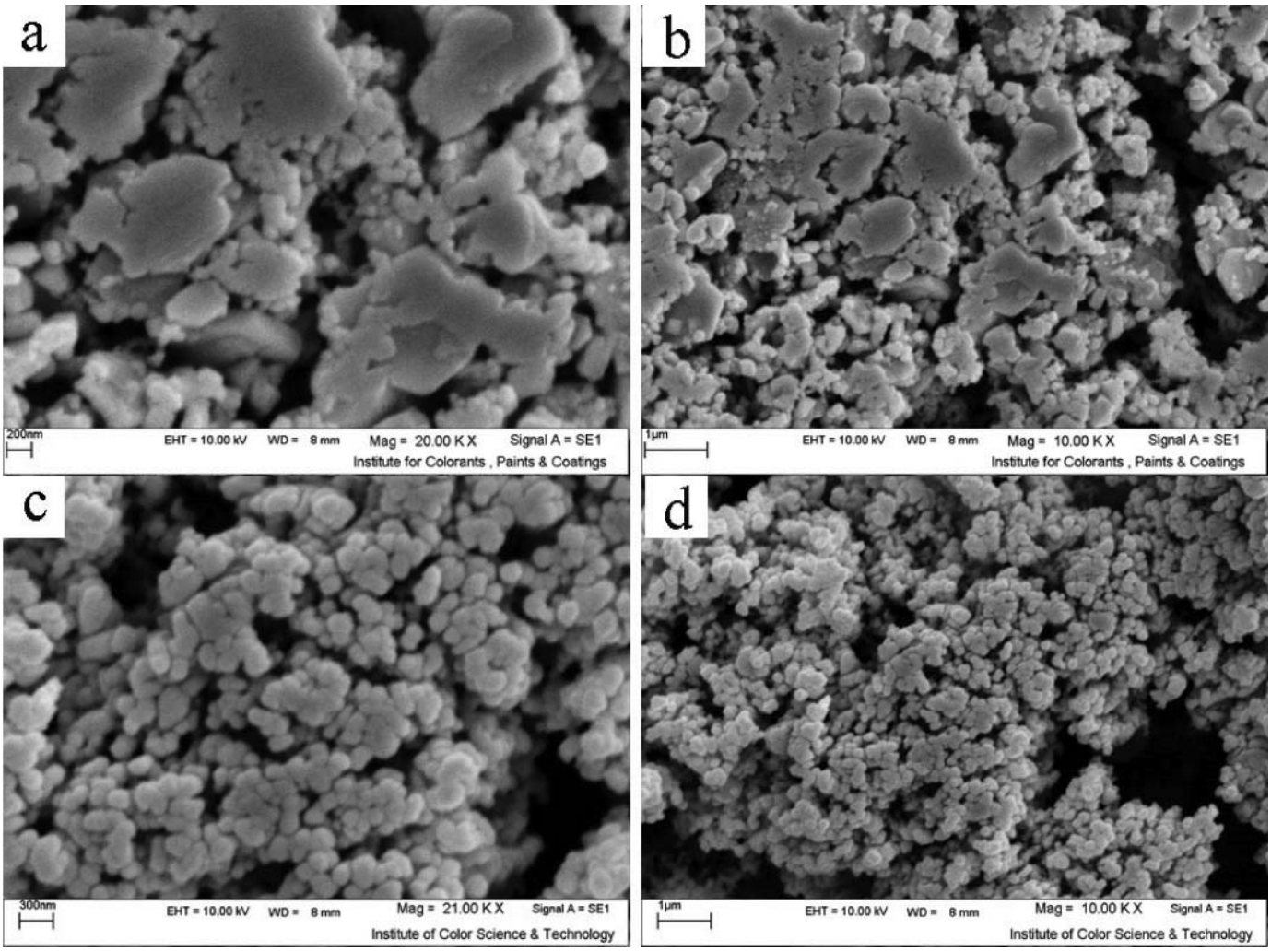

Fig. 2. SEM images of prepared samples in the: (a and b) presence of $AgNO_3$ (sample no. 1), (c and d) presence of [Ag(HSal)] (sample no. 2).

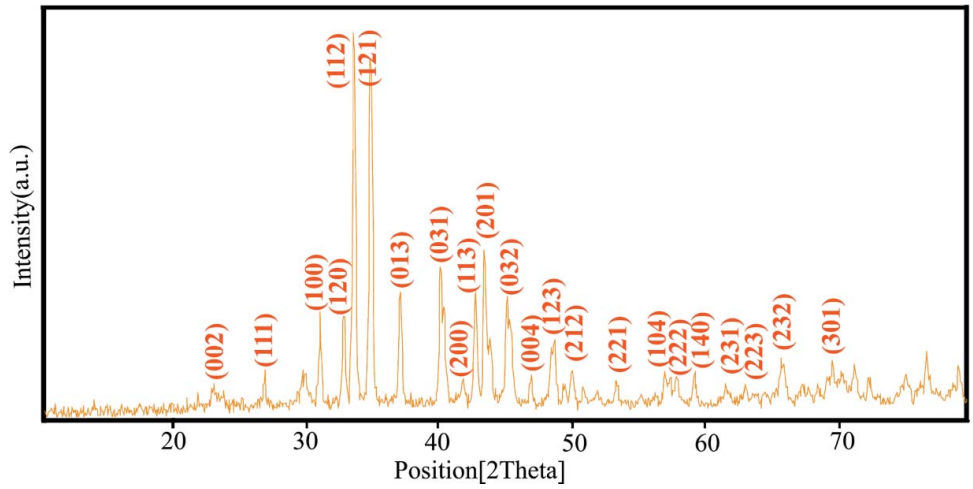

Fig. 3. XRD patterns of sample no. 2.

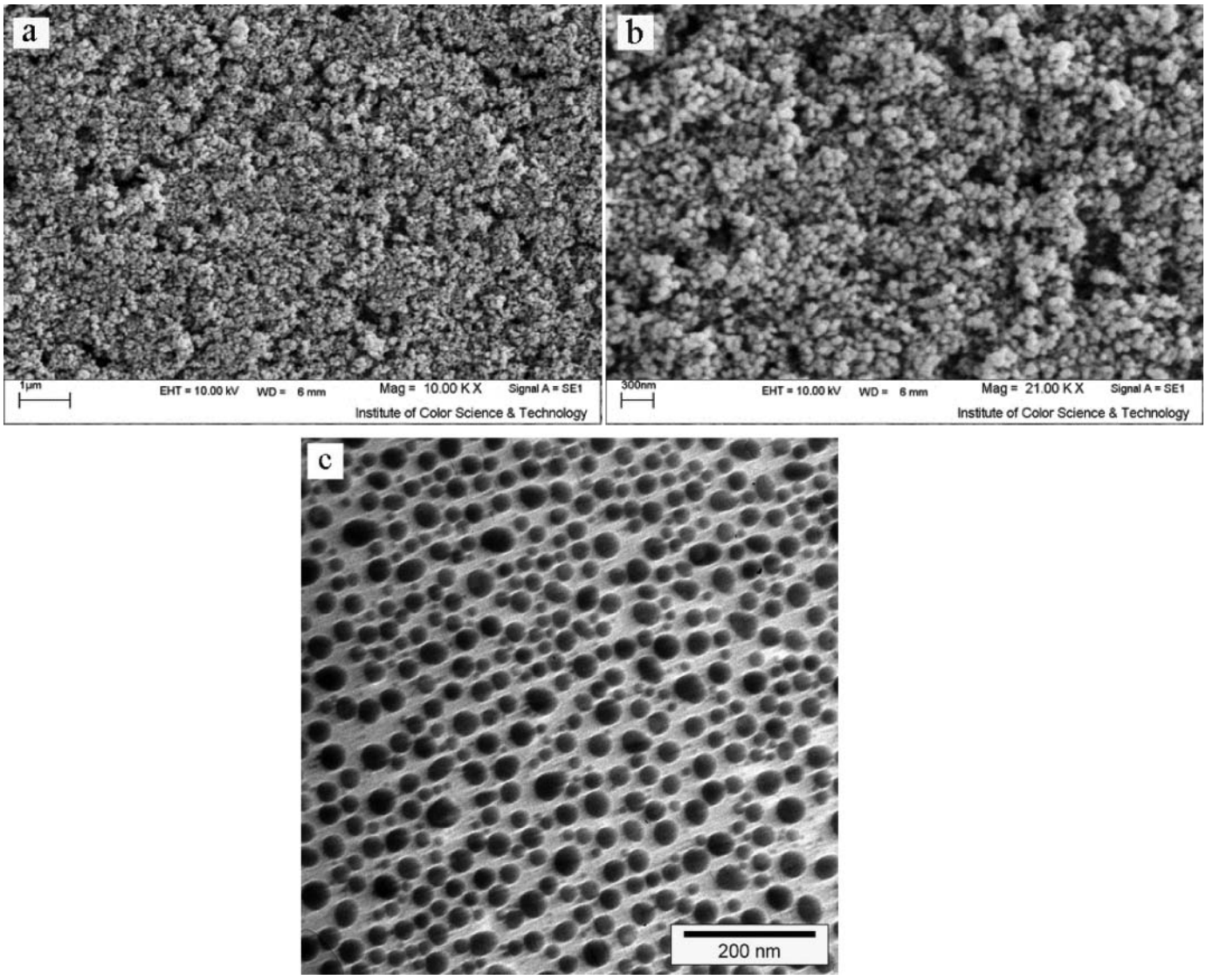

Fig. 4. (a and b) SEM and (c) TEM images of prepared sample in the pH = 10 (sample no. 3).

good crystallinity of the nanoparticles and the peak broadening is due to the small size of nanoparticles.

The effect of pH on morphology and particle size of Ag_2Se sample is shown in Figure 4. The morphology and structure of the resulting samples were investigated by SEM and TEM images. For this purpose, reactions were carried at in two different pH values. It can be observed that with increasing pH from 5 (sample no. 2; Figure 2) to 10 (sample no. 3; Figure 4) the size and agglomeration of the nanoparticles were decreased. The pH of reaction was adjusted to 10 by adding aqueous solution of $NaHCO_3$ 0.1 M to the [Ag(HSal)] solution. Increasing the pH resulted in smaller and more uniform nanoparticles with narrow size distribution. It is suggested that the bicarbonate anions encircle the Ag ions, therefore can play surfactant role in the reaction medium. Figure 4 shows the TEM image of Ag_2Se nanoparticles with diameters between 20 and 30 nm.

In the preparation of Ag_2Se, different ultrasonic powers were applied. If the ultrasonic power was increased, the extent of the collapse of the bubble would be greatly increased, leading to a higher temperature and pressure accordingly, which would enhance the effect of ultrasonic chemical reaction as a whole.[32] Increasing the variation ultrasound power increases acoustic pressure so it makes cavitation phenomenon increased. Hence, the particle size will decrease due to the increased cavitation effect.[33] Figure 5 shows the SEM images of the Ag_2Se samples which prepared in the presence of two different ultrasound powers 55W/cm^2 and 65 W/cm ^{2}. It can be observed that when ultrasound power was 55 W/cm^2, the agglomeration of nanoparticles decreased (Figure 5). So it was found that 55 W/cm^2 was the optimum power. The effects of reaction temperature in sonochemical method on the morphology and shape of Ag_2Se samples in the optimum ultrasound power are shown in

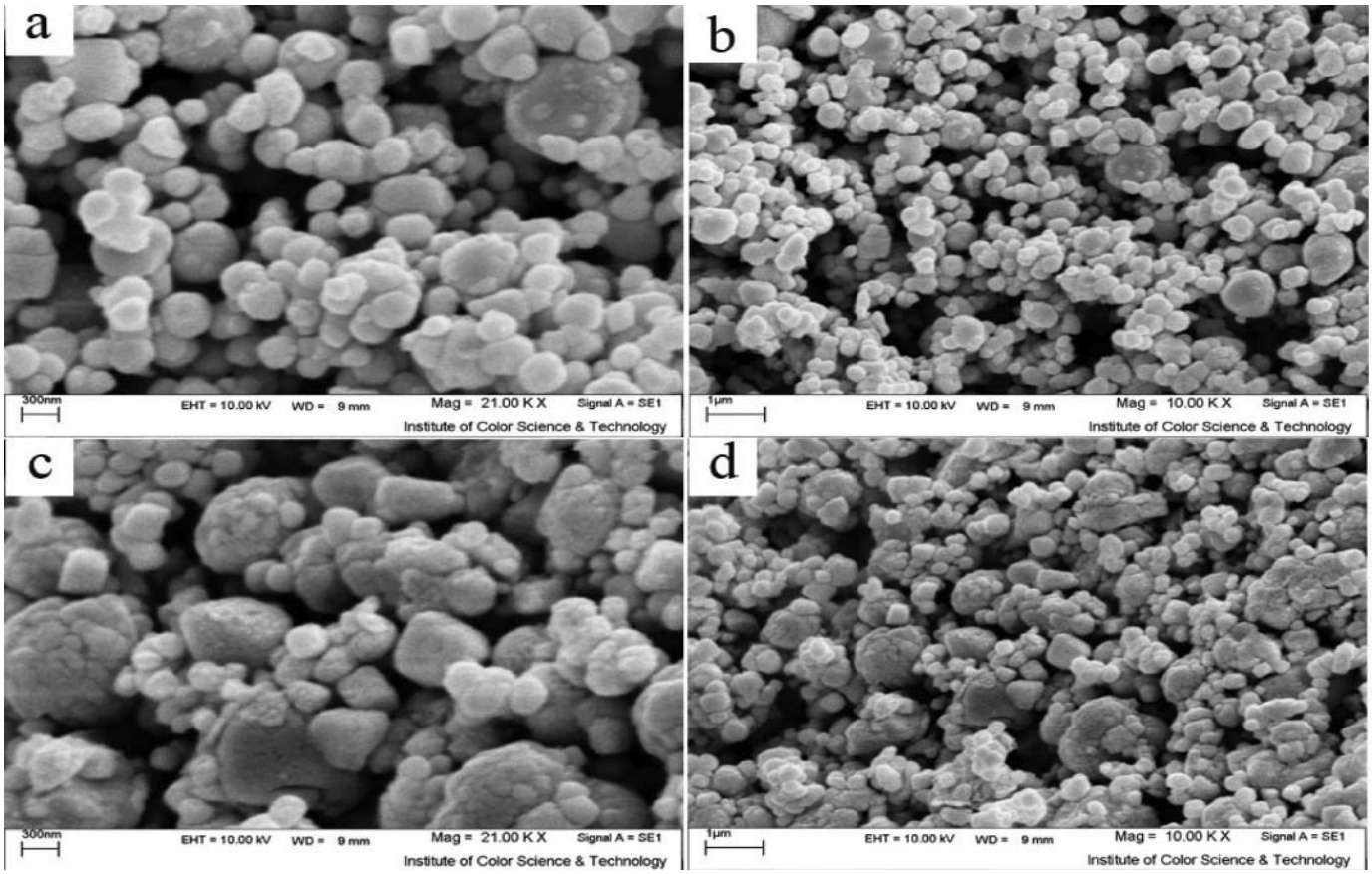

Fig. 5. SEM images of prepared samples in the presence of different sonication power: (a and b) 55 W/cm^2 (sample no. 4), (c and d) 65 W/cm ^{2} (sample no. 5).

Figure 6. For this purpose reactions were carried out in four different temperatures. It can be observed that with increasing temperature from room temperature (25°C; Figure 5) to 45°C (Figure 6), and to 65°C (Figure 6), the size and agglomeration of the nanoparticles were decreased, whereas with decreasing temperature from 25°C to 10°C (Figure 6) the agglomeration of nanoparticles was increased. Indeed, temperature affects the sonochemical reaction rate, therefore low temperatures cause a higher viscosity, which makes the formation of the bubble more difficult.

Upon increasing the mole ratio of [Ag (HSal)] and $SeCl_4$ to 2:1 (sample no. 9) the high-magnification SEM image in Figure 7, indicates that the size and agglomeration of nanoparticles were increased and spherical particles were formed. In fact, concentration of reactants could change the morphology of products. EDS technique was employed to investigate the chemical composition and purity of as-synthesized Ag_2Se nanoparticles. The EDS pattern (Figure 8) confirms the presence of Ag and Se in sample no. 2. In addition, no O, C, or N signals are detected in the spectrum.

The UV-Vis absorption spectrum of Ag_2Se (sample no. 2) is shown in Figure 9. The figure shows a strong absorption at 280 nm. Figure 9 shows that the band gap of Ag_2Se nanoparticle (sample no. 2) is 2.45 eV, which shows a blue shift compared to that of bulk Ag_2Se (0.15 eV), indicating a quantum size effect.[33] To investigate the effect of ultrasound irradiation on the morphology and particle size of the products, the experiment was carried out under mechanical stirring conditions (sample no. 10). The SEM image of sample no. 10 is shown in Figure 10. It is clear that aggregated nanostructures were formed in the absence of sonication (Figure 10).

Figure 11 shows the XRD pattern of sample no. 10. The sample was found to be a mixture of Ag (JCPDS card no. 87-0718), Se (JCPDS card no. 42-1425), and Ag_2Se (JCPDS card no. 24-1041) phases. As a result, the expected pure products could not be obtained under mechanical stirring conditions.

According to the previously mentioned results, the ultrasound-assisted method is an appropriate point to synthesis Ag_2Se nanoparticles. An ultrasound wave has an important role to produce cavitation and it can do advanced chemical reactions such as: oxidation, reduction, dissolution, and decomposition.[34] According to the blank test, it was found that the stirring has weak effect on the Se^{4+} and hydrazine degradation. in addition, some of Ag^+ ions can react with

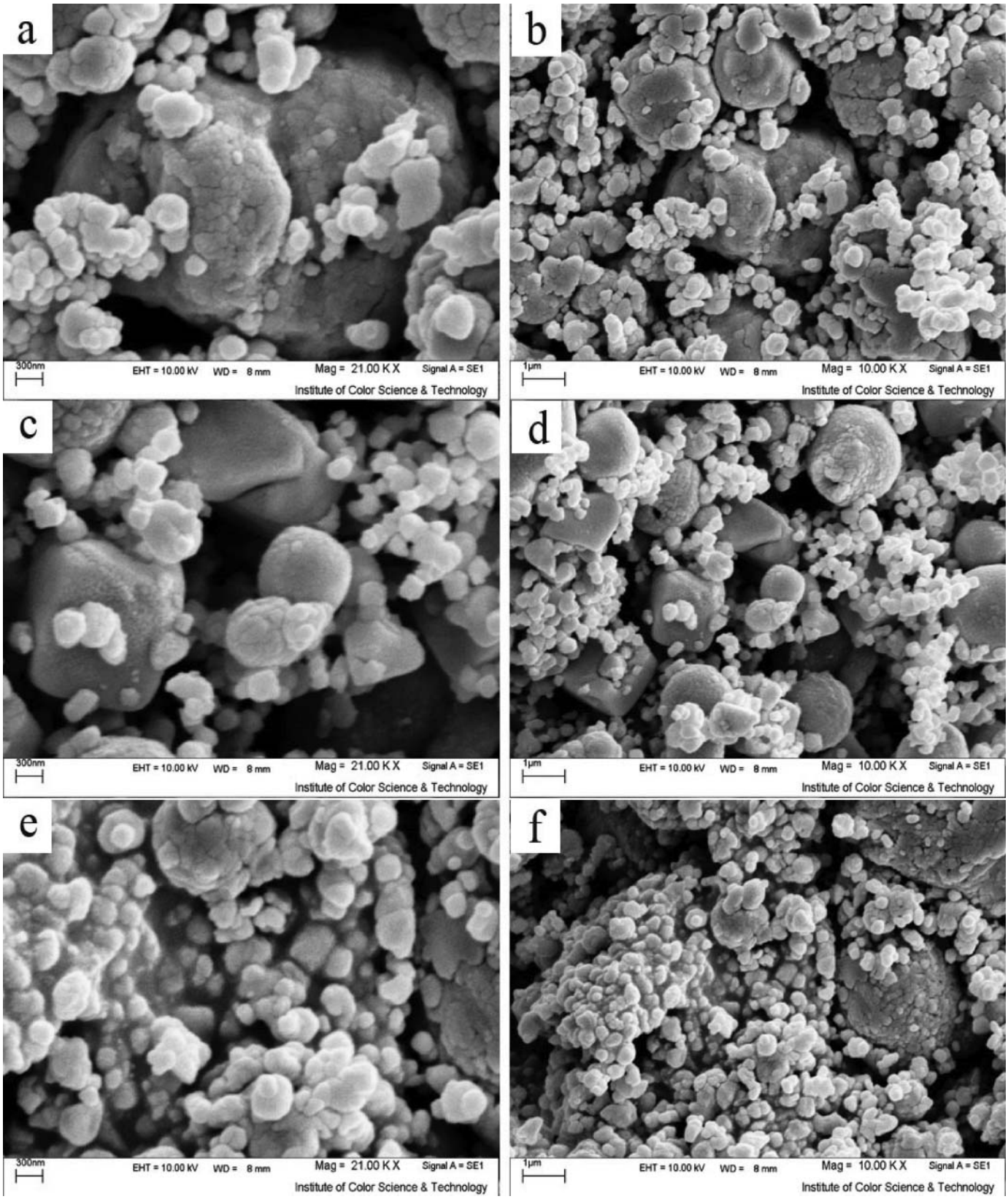

Fig. 6. SEM images of prepared samples in the presence of different sonication temperature: (a and b) 10°C (sample no. 6), (c and d) 45°C (sample no. 7), (e and f) 65°C (sample no. 8).

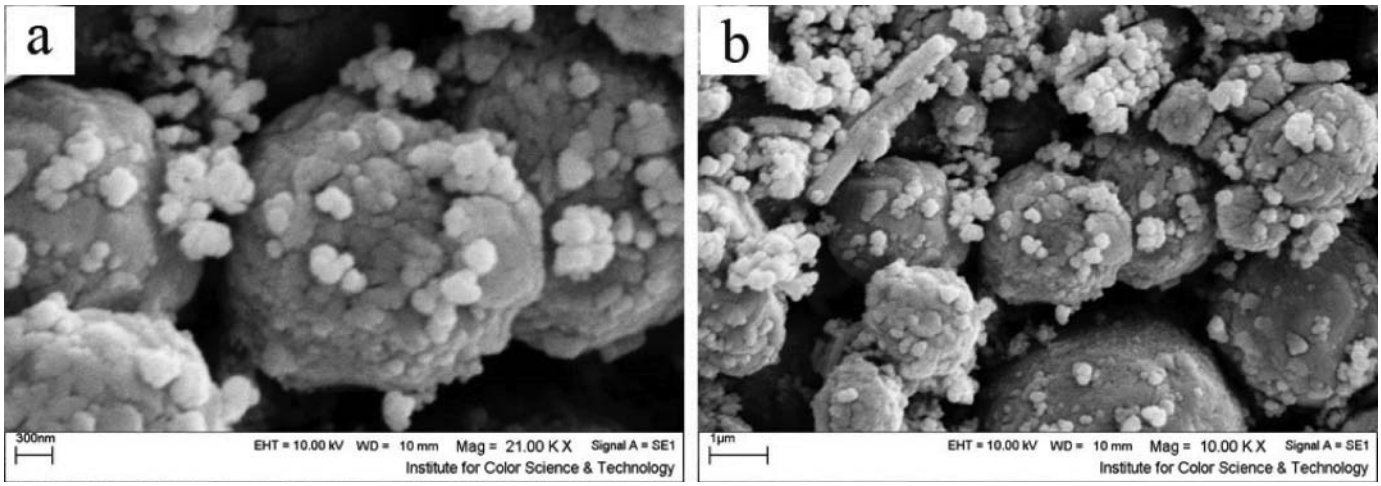

Fig. 7. SEM images of prepared sample for which the molar ratio of Ag/Se is 2:1 (sample no. 9).

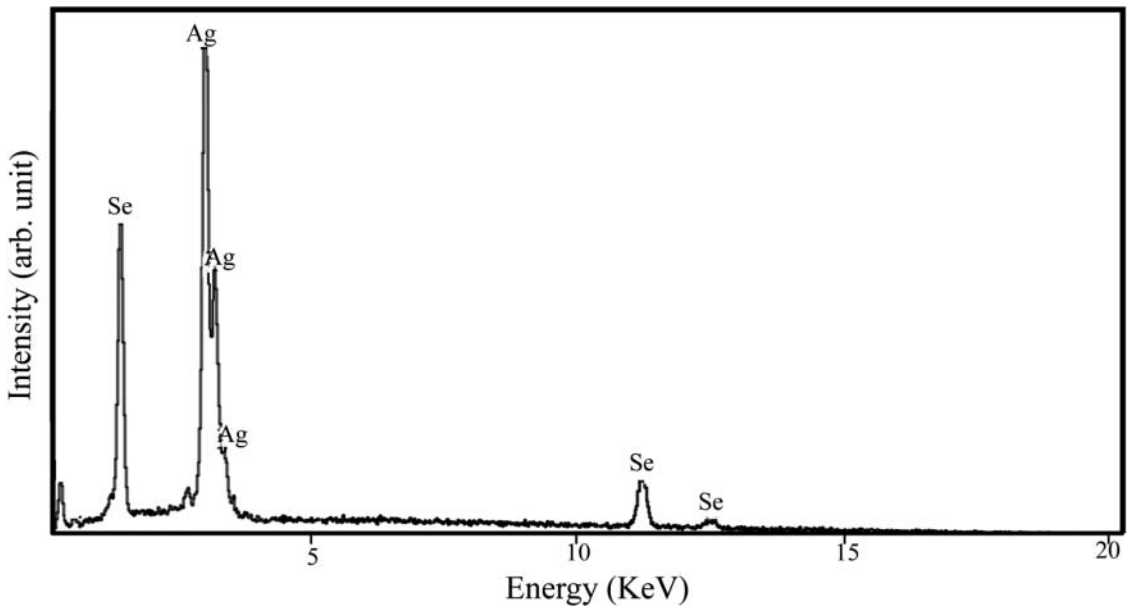

Fig. 8. EDS pattern of Ag_2Se (sample no. 2).

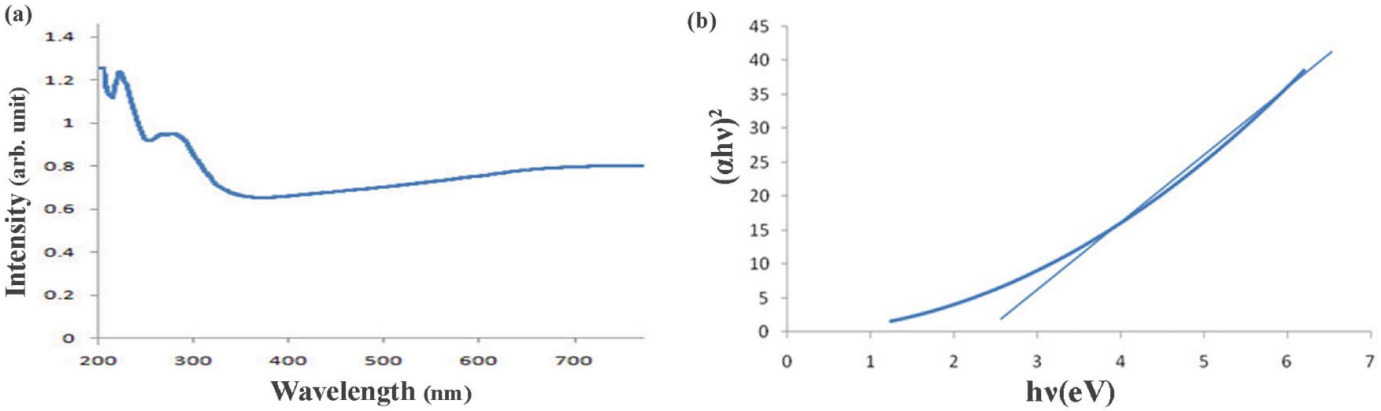

Fig. 9. (a) UV-Vis spectrum of Ag_2Se (sample no. 2). (b). Optical absorption plots of $(\alpha h\nu)^2$ versus photon energy ($h\nu$).

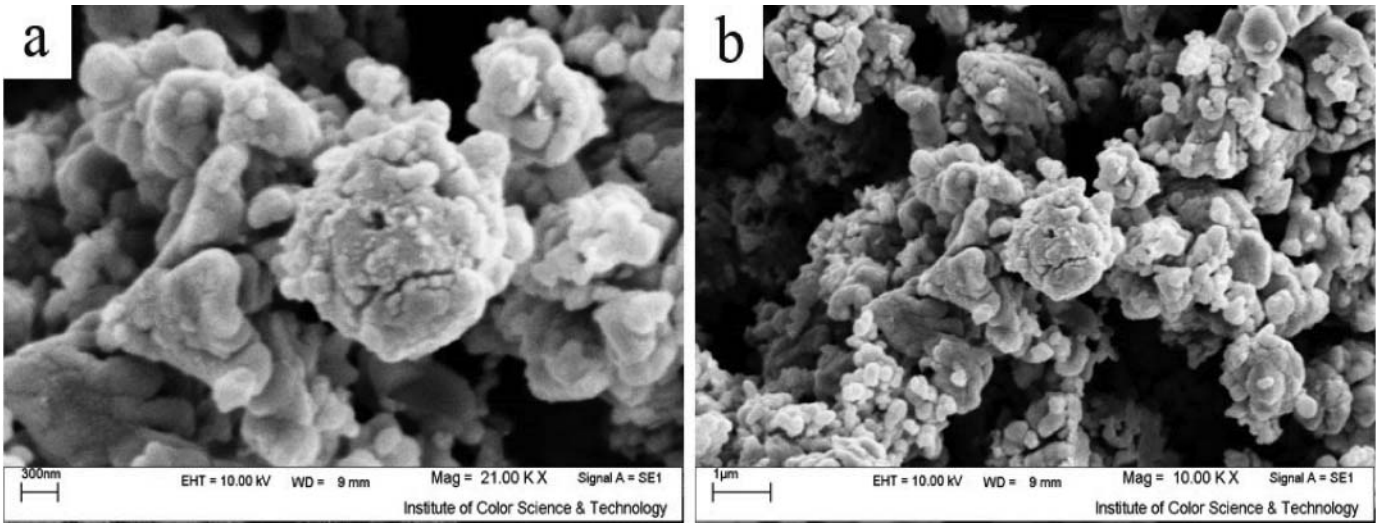

Fig. 10. SEM images of bulk sample(sample no. 10).

residual hydrazin in the reaction medium, hence Ag^+ ions were reduced to Ag^0. The formation of H_2O_2 and H_2 has been known to take place during sonochemical reactions.[35]

$$H_2O \rightarrow H + OH$$
$$H + H \rightarrow H_2$$
$$H + OH \rightarrow H_2O_2$$

The plausible formation process of Ag_2Se can be summarised as follows[36]:

$$[Ag(HSaL)] + H_2O \rightarrow Ag^+_{(aq)} + HSaL^-_{(aq)}$$
$$SeCl_4 + 3H_2O \rightarrow H_2SeO_3 + 4HCl$$

Hydrazine hydrate is freely soluble in water, but since N_2H_4 is basic, the chemically active free-ion is normally represented as $N_2H_5{}^+$[37]:

$$N_2H_4H_2O \rightleftharpoons N_2H_5^+ + OH^-$$
$$N_2H_5^+ \rightleftharpoons N_2 + 5H^+ + 4e^-$$

So

$$H_2SeO_3 + N_2H_5^+ \rightarrow Se^0 + N_2 + 3H_2O + H^+$$

under ultrasound irradiation, Se^0 can be reduced to Se^{-2}. Furthermore, the ultrasound wave induces the oxidation of

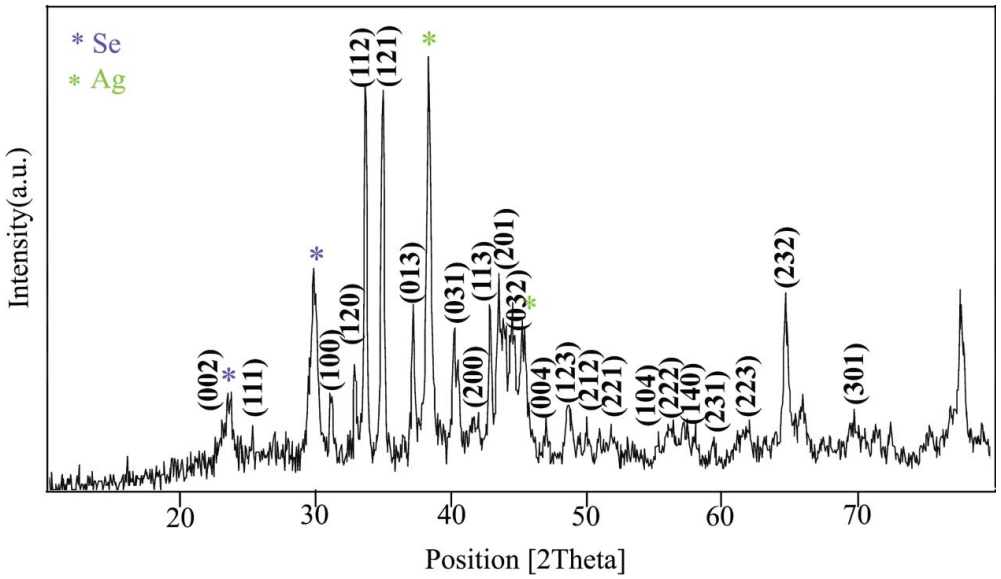

Fig. 11. XRD patterns of bulk sample (sample no. 10).

Ag^0.[29] Therefore, in the absence of ultrasound irradiation no pure product can be achived.

$$Se^0 + H_2 \rightarrow Se^{2-} + 2H^+$$
$$4Ag^+ + N_2H_5^+ \rightarrow 4Ag^0 + N_2 + 5H^+$$

Ag^0 was oxidized to Ag^+ ions:

$$2Ag^0 + H_2O_2 \rightarrow 2Ag^+ + 2OH^-$$
$$2Ag^+ + Se^{2-} \rightarrow Ag_2Se$$

Conclusions

In summaray, Ag_2Se nanoparticles were synthesized via sonochemical route using new precursors. There are no reports on the prepration silver selenide whitout using capping agent but we attempted to employ the simple method to prepare Ag_2Se. Thus, this work is the only successful sonochemical synthesis of silver selenide nanostructures from silver salicylate. According to the blank test, ultrasound irradiation plays important role to prepration Ag_2Se nanoparticles. The effects of different parameters, such as pH, reaction tempreture, ultrasound power, and mole ratio of precursors on the morphology of products were investigated. This method brings forward a broad idea to synthesize other metal selenides from inorganic precursors.

Funding

Authors are grateful to Council of University of Kashan for providing financial support to undertake this work by Grant No. 159271/78.

References

1. Kobayashi, M. *J. Solid State Ionics.* **1990**, *39*, 121.
2. Ferhat, M.; Nagao, J. *J. Appl. Phys.* **2000**, *88*, 813.
3. Schoen, D. T.; Xie, C.; Cui, Y. *J. Am. Chem. Soc.* **2007**, *129*, 4116–4117.
4. Liang, Y. C.; Tada, K. *J. Appl. Phys.* **1988**, *64*, 4494.
5. Hodes, G.; Manassen, J.; Cahen, D. *Nature* **1976**, *261*, 403.
6. Santhosh Kumar, M. C.; Pradeep, B. *J. Semicond. Sci Technol.* **2002**, *17*, 261.
7. Harpeness, R.; Palchik, O.; Gedanken, A.; Palchik, V.; Ameil, S.; Slifkin, M. A.; Weiss, A. M. *J. Chem. Mater.* **2002**, *14*, 2094.
8. Sahu, A.; Qi, L.; Kang, M.; Deng, D.; Norris, D. *J. Am. Chem. Soc.* **2011**, *133*, 6509.
9. Manoharan, S.; Prasanna, S.; Kiwitz, D.; Schneider, C. *Phys. Rev.* **2001**, *63*, 2124051.
10. Ohtani, T.; Motoki, M. *J. Mater. Res. Bull.* **1995**, *30*, 1495.
11. Stuczynski, S.; Brennan, J.; Steigerwald, M. *J. Inorg. Chem.* **1989**, *28*, 4431.
12. Cheon, J.; Zink, J. I. *J. Am. Chem. Soc.* **1997**, *119*, 3838.
13. Su, H.; Xie, Y.; Li, B.; Qian, Y. *Mater. Res. Bull.* **2000**, *35*, 465.
14. Chen, R.; Xu, D.; Guo, G.; Gui, L. *J. Electrochem. Commun.* **2003**, *5*, 579.
15. Li, B.; Xie, Y.; Huang, J.; Qian, Y. *Ultrason. Sonochem.* **1999**, *6*, 217.
16. Khanna, P. K.; Singh, N.; Charan, S.; Patil, K. R. *Mater. Lett.* **2006**, *60*, 2080.
17. Wang, H.; Qi, L. *Adv. Funct. Mater.* **2008**, *18*, 1249.
18. Mohanty, B. C.; Malar, P.; Osipowicz, T.; Murty, B. S.; Varmad, S.; Kasiviswanathan, S. *Surf. Interface Anal.* **2009**, *41*, 170.
19. An, B. H.; Ji, H. M.; Wu, J. H.; Cho, M. K.; Yang, K. Y.; Lee, H.; Kim, Y. K. *Curr. Appl. Phys.* **2009**, *9*, 1338.
20. Woods, M. E.; Krieger, I. M. *J. Colloid Interface Sci.* **1970**, *34*, 91.
21. Suslick, K. S. *Science* **1990**, *247*, 1439.
22. Doktycz, S. J.; Suslick, K. S. *Science* **1990**, *247*, 1067.
23. Soofivand, F.; Mohandes, F.; Salavati-Niasari, M. *Micro Nano Lett.* **2012**, *7*, 283.
24. Soofivand, F.; Mohandes, F.; Salavati-Niasari, M. *Mater. Lett. Bull.* **2013**, *48*, 2084.
25. Salavati-Niasari, M.; Javidi, J.; Davar, F.; Amini-Fazl, A. *J. Alloys Compd.* **2010**, *503*, 500.
26. Salavati-Niasari, M.; Hosseinzadeh, G.; Davar, F. *J. Alloys Compd.* **2011**, *509*, 4098.
27. Pejova, B.; Grozdanov, I. *Mater. Lett.* **2004**, *58*, 666.
28. Mason, T. J.; Lorimer, J. P.; Bates, D. M. *Ultrasonics* **1992**, *30*, 40.
29. Mohandes, F.; Salavati-Niasari, M. *Sonochem.* **2013**, *20*, 354
30. Haines, P. J. *Principles of Thermal Analysis and Calorimetry*; The Royal Society of Chemistry, London, 2002.
31. Emadi, H.; Salavati-Niasari, M.; Davar, F. *MicroNano Lett.* **2011**, *6*, 909.
32. Ding, T.; Zhu, J.-J.; Hong, J.-M. *Mater. Lett.* **2003**, *57*, 4445.
33. Anthony, S. P. *Mater. Lett.* **2009**, *63*, 773.
34. Manoiu, V.-S.; Aloman, A. *U.P.B. Sci. Bull.* **2010**, *72*, 1454.
35. Suslik, K. S. editor. *Ultrasound: Its Chemical, Physical And Biological Effects*; VCH, Weinheim, Germany, 1988.
36. Henglein, A.; Korman, C. *Int. J. Radiat. Biol.* **1985**, *48*, 251.
37. Esmaeili-Zare, M.; Salavati-Niasari, M.; Sobhani, A. *Ultrason. Sonochem.* **2012**, *19*, 1079.